

A parameterized 2D Quasi-Geostrophic model of thermal convection in a rapidly rotating spherical shell

Gonzalo Rubio

Department of Physics, University of Alberta, Edmonton, AB, Canada

Abstract

Planetary flows involving the balance of pressure gradients and the Coriolis force are termed geostrophic. This is an idealized model since convective flows are rarely purely geostrophic because of buoyancy and viscous dissipation. Thus, we call such flows, Quasi-Geostrophic flows. The Quasi-Geostrophic approach is supported by the Taylor-Proudman theorem, which states that a rapidly rotating fluid will be nearly invariant in the axial direction. Furthermore, compressibility will be ignored, except where density variations lead to buoyancy forces, which positions us within the Boussinesq approximation. Previous parameterized 2D QG models limit buoyancy, which plays a huge role in convection, to its equatorial component and the modeled region of convection is restricted to outside of the tangent cylinder. Though these models faithfully reproduce some features of three-dimensional numerical models, we wish to include the axial component of buoyancy and extend the modeled region of convection inside of the tangent cylinder. Here, we verify a prolonged 2D which can capture the leading order dynamics of the full 3D thermal convection in a rapidly rotating spherical shell. The topmost advantage of such QG models is that, because of their simplified structure, a higher resolution is more easily attainable than for 3D models for the same or even less computing power and can thus be exploited to capture fundamental aspects of thermal convection which may be otherwise quite complicated. The model presented can successfully replicate the prominent features of 3D numerical models near onset of thermal convection.

1. Introduction

Convective heat transfer or thermal convection is the physical transfer of heat in space caused by the movement of fluids. Convection can be caused by natural buoyancy forces and are responsible for the mechanical motion when the fluid is either cooled or heated.

Numerical models of thermal convection in rapidly rotating spheres have been the subject of many papers, mainly due to their relevance in the physics of planetary interiors (J. Schmalzl et al. 2004). In general, planetary flows are confined to rapidly rotating concentric spheres and dictate the thermal evolution of planetary bodies. Some examples of thermal convection in our Solar system include the convection zone of the Sun in which Heat is carried in columnar manner and these convective regions can cause small magnetic fields (Savchenko et al. 1978). Thermal convection also occurs in the mantle of Terrestrial planets, this is best appreciated by looking at the Earth's dynamic topography which is a current expression of mantle convection (Conrad, C. P. 2002). The subject has also gained interest as a model for the generation of magnetic fields from self-sustained dynamos in electrically conducting fluid planetary cores (A. M. Soward, 1974). It has also gained interest as a source for large zonal flows observed on Gas giants (K. Soderland, J. Aurnou, 2007), for surface winds of ice giants (F. Sohl et al. 2010), and for the cause of hotspot volcanism from deep rocky interiors of icy satellites (G. W. Ojakangas, D. J. Stevenson, 1986).

While geostrophic motion would arise from the exact balance of the Coriolis force and horizontal gradient forces, the term Quasi-Geostrophic or QG for simplicity, results these forces being "almost" in balance because of introducing small perturbations with respect to the fundamental state.

Although this experiment seems to be mainly theoretical, it has meteorological practical applications here on Earth. For instance, the may public wish to know information regarding temperature, humidity, precipitation, wind speed and direction for a geographic region up to a week in advance. Based on the integration of the fundamental QG equations forward in time we can predict the likelihood of certain meteorological events.

The main concern of this experiment is to build a Quasi-Geostrophic model that successfully reproduces the key aspects of thermal convection that a full 3D model would produce. Such model, if successful, will aid in the diagnose of the spatial and temporal evolution of 3D synoptic scale weather systems.

Parameterized numerical models of thermal convection in which the full problem is reduced to 2 dimensions have the potential to lead the way towards developing less computationally demanding, faster, higher temporal and spatial resolution thermal convection in such geometry.

2. Theoretical frame work

2.1 Geometry

For our study, we will limit ourselves to a Boussinesq fluid confined within a rotating spherical shell, Figure 1 gives a detailed view of the geometry and notations. The whole approach aims at describing the motion outside and inside the tangent cylinder.

In a spherical shell geometry, we are concerned with four regions. Two regions of great interest involve the volume of fluid enclosed by a tangent cylinder circumscribing the equatorial plane of the inner sphere, as well as the volume outside such tangent cylinder. For simplicity, we will refer to the tangent cylinder as TC. The other two regions of interest are the north and south regions within the TC. The form of convection should depend whether we are located inside or outside the tangent cylinder since the gravity and rotation vector align differently depending on the region (Figure 2). As we know this is crucial in determining the type of flow since it heavily depends on rotation. Additionally, one should consider whether we are in a thick or thin shell regime as the volume either outside or inside the TC will be different, thus dictating whether we will mainly observe axial plumes or columnar rolls.

Outside the TC, such vectors are approximately perpendicular to each other, whilst inside the TC, they are almost parallel to each other. For the first case, flows are expected to rigid and take the form of columnar rolls with flow components perpendicular to rotation. For the later, one would expect Rayleigh-Benard convection with energy carrying axial plumes, coupled with non-rigid horizontal flows (Figure3).

Rotation imparts a two-dimensionality on flows since horizontal flows are assumed to be axially invariant, so they can be properly represented on an equatorial plane. Temperature anomalies are also assumed to be axially invariant. Axial flows lead to vortex stretching and are not neglected in the model. Inside the TC, axial plumes and anti-symmetric horizontal flows though not rigid, they are still constrained by the leading order force balance of the Coriolis force and pressure gradients, thus can still be referred to as QG flows. In order to extend existing QG models to regions inside the TC, the geometry must be modified. Whilst the top and bottom of

the columnar rolls are in contact with the outside sphere outside the TC, they are in contact with both the inside and outside spheres for flows inside the TC, which have different radii and curvature (Figure 4). More importantly, to include the axial component of buoyancy, one must track the evolution of axial flows, non-rigid horizontal flows and non-rigid temperature perturbations.

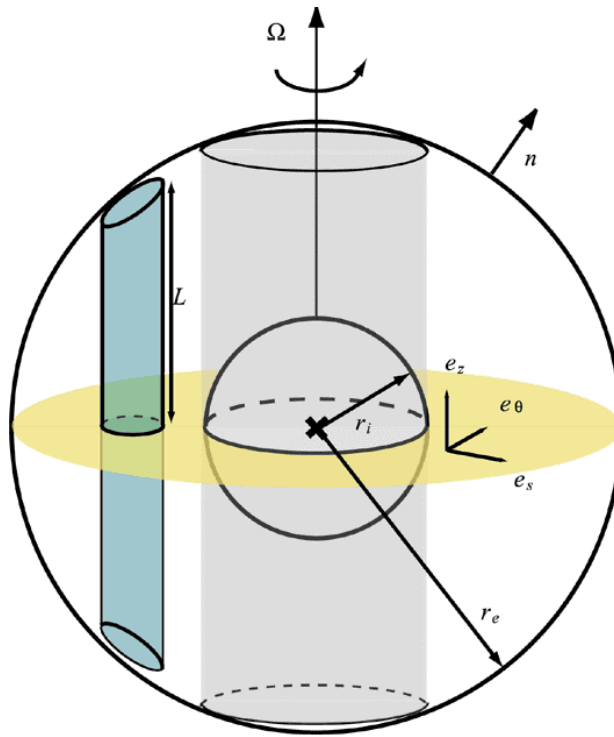


Figure1. Sketch of the geometry of the problem. Radii of concentric shells noted, unit normal to the surface, angular velocity of rotation about its axis, outside and inside tangent cylinder regions noted as well. Fluid motion is solved in the equatorial plane, assuming a vertical column for convective cells. Modified from figure 1 Julien Aubert, et al. 2003.

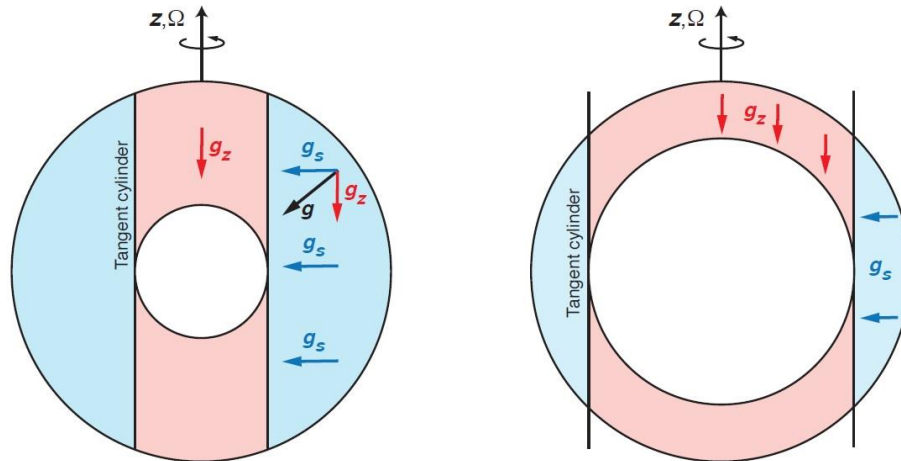


Figure 2. Schematic representation of fluid volume occupying the convective regions inside and outside the TC for a thick (right) and thin (left) shell geometry. Rotation and gravitational vectors are to first order aligned with each other inside the TC and are normal to each other outside the TC. Furthermore, inside the TC, the region above the inner shell will differ only from the bottom by a opposite orientation of the gravitational vector. Modified from Figure 1 Dumberry at al. 2015.

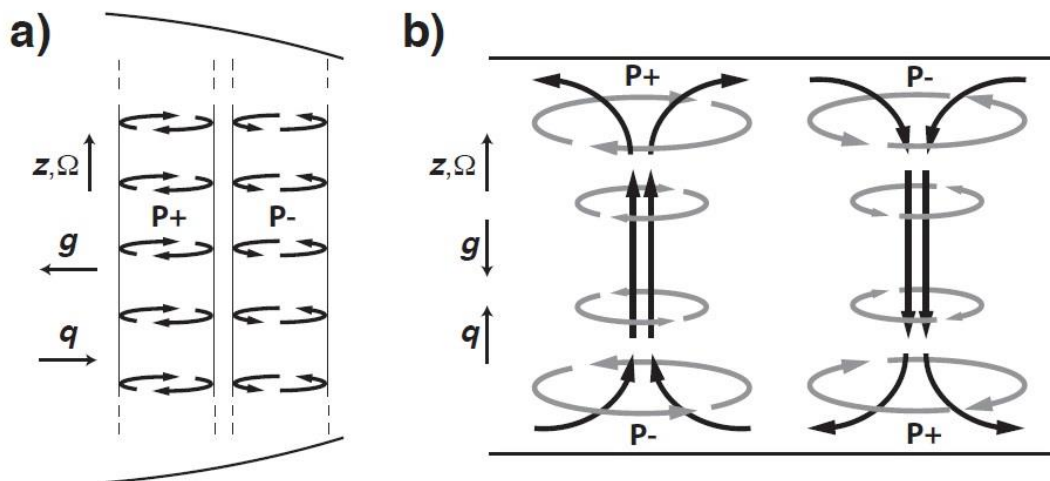


Figure3. Geometry of thermal convection for regions inside and outside the TC.

- a) Outside The TC, gravity being mainly normal to rotation will cause heat flow to be horizontal and axially invariant. Such flow is said to be Toroidal.
- b) Heat will be carried by axial plumes in response to gravity being mainly parallel to the axis of rotation. Such flow is said to be poloidal.

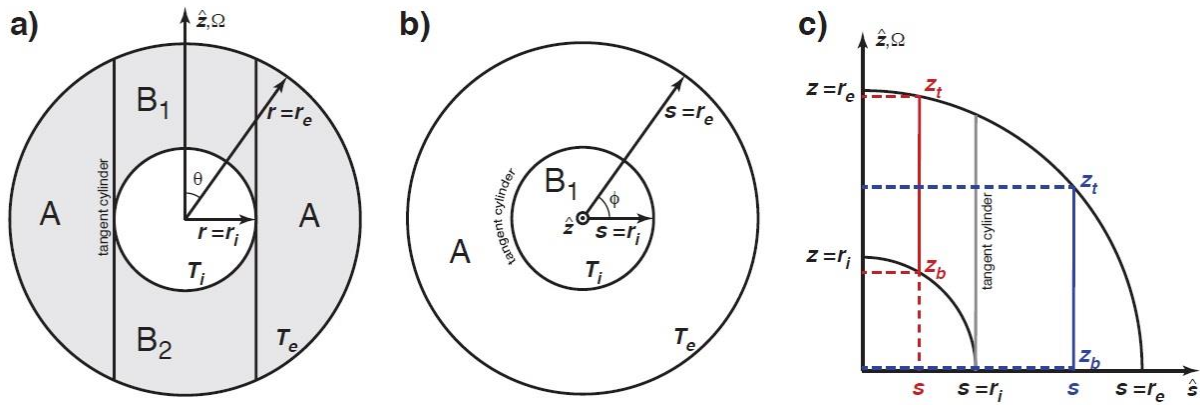


Figure 4. Figure modified from figure 3 Dumberry et al., 2015

- a) Meridional slice of the problem geometry. The convective fluid will be restricted between the inner and outer radii. The fluid can be further separated into three volumes, outside the TC (A) and inside the TC (B).
- b) Longitudinal cross-section representing the parameterized 2D domain. For simplicity, only the northern hemisphere is simulated and will be given by axial averages, since the bottom hemisphere differs only by a negative sign, though convection patterns will be very similar.
- c) Meridional slice showing the geometry of the fluids inside and outside the TC. Inside the TC, the bottom and top of fluids will be in contact with shares of different curvature. Alternatively, outside the TC, the fluid will always be constrained between the outer sphere.

2.2 Fundamental equations

The mathematics behind quasi-geostrophic flows are quite complex and extensive. Since our objective is to simply verify the validity of the parameterized model developed by Dr. Dumberry et al., I will only attempt to lay an oversimplified mathematical foundation of the problem by only mentioning the most relevant equations and parameters governing QG flows.

Due to the symmetry of the problem, we will use either spherical or cylindrical coordinates to represent a specific location given by (r, θ, ϕ) or (s, ϕ, z) respectively.

In our case, thermal convection will be governed by the Navier-Stokes and temperature equations

$$\frac{\partial \mathbf{u}}{\partial t} + (\mathbf{u} \cdot \nabla) \mathbf{u} + 2\hat{\mathbf{z}} \times \mathbf{u} = -\nabla p + E \nabla^2 \mathbf{u} + Ra^* \Theta g_r \hat{\mathbf{r}} \quad (1)$$

$$\frac{\partial \Theta}{\partial t} + \mathbf{u} \cdot \nabla (T + \Theta) = \frac{E}{Pr} \nabla^2 \quad (2)$$

Along with the incompressibility condition

$$\nabla \cdot \mathbf{u} = 0 \quad (3)$$

Here, \mathbf{u} is the flow, p represents pressure, Θ is the temperature perturbation from either cooling or heating at the boundaries. These equations are non-dimensional since we use Ω_0^{-1} as the typical length as time, and the temperature contrast within the shell $\Delta T = T_i - T_e$ as the temperature scale. E is the Ekman number, Pr is the Prandtl number and Ra^* is a modified Rayleigh number, all of which are given by

$$E = \frac{\nu}{\Omega_0 r_e^2} \quad Pr = \frac{\nu}{\kappa} \quad Ra^* = \frac{Ra E^2}{Pr} \quad Ra = \frac{\alpha \Delta T g_0 r_e^3}{\nu \kappa} \quad (4)$$

The dynamics of thermal convection are governed mainly by three dimensionless parameters. The Ekman number which describes the ratio of viscous forces to Coriolis forces arising from planetary rotation. In our experiment, we considered ($E \ll 1$) which allows perturbations to propagate Due to low frictional values. The Rayleigh number (Ra), which describes the instability of a layer of fluid bound by layers at the top and bottom which have temperature induced density variations. This parameter is the one which we are most interested in since it tells us about the onset of convection, and at which critical value this happens. Thus, the experiment revolves around keeping everything else constant while increasing the Rayleigh number. Lastly, the Prandtl number (Pr) which is the ration between the kinematic viscosity ν and thermal diffusivity κ . The simplest model for such parameter, is the Reynold's analogy which assumes heat flux and momentum flux are equivalent in a turbulent system, meaning the ratio must be constant for all positions independent of radius. Reynold's analogy yields a Prandtl number equal to the unity, this will in turn normalize velocities and temperatures.

Additionally, the gravitational acceleration, can be written in cylindrical coordinates as

$$g_r \hat{r} = g_s \hat{s} + g_z \hat{z} \quad (5)$$

By taking the curl of Eq. (1), one will obtain an expression for the vorticity

$$\frac{\partial \boldsymbol{\omega}}{\partial t} - (\boldsymbol{\omega} \cdot \nabla) \mathbf{u} + (\mathbf{u} \cdot \nabla) \boldsymbol{\omega} - \frac{2\partial u}{\partial z} = E \nabla^2 \boldsymbol{\omega} + Ra^* \nabla \nabla (\Theta g_r \hat{r}) \quad (6)$$

Under our assumption of rapidly rotating sphere or in other words a small Ekman number ($E \ll 1$), the balance between the Coriolis force, pressure gradient and buoyancy is given by

$$2\hat{z} \nabla \mathbf{u} = -\nabla p + Ra^* \Theta g_r \hat{r} \quad (7)$$

Similarly, when pressure gradients are ignored in the vorticity equation, the leading order balance of Eq. (6) is

$$-\frac{2\partial u}{\partial z} = Ra^* \nabla \nabla (\Theta g_r \hat{r}) \quad (8)$$

In Eqs. (7) and (8), \mathbf{u} is most easily expressed by

$$\mathbf{u} = \mathbf{u}_\perp + u_z \hat{z} \quad (9a)$$

Where \mathbf{u}_\perp is the perpendicular component of flow relative to the rotation axis

$$\mathbf{u}_\perp = u_s \hat{s} + u_\phi \hat{\phi} \quad (9b)$$

In an analogous manner, the vorticity is given by

$$\boldsymbol{\omega} = \boldsymbol{\omega}_\perp + \omega_z \hat{z} \quad (10)$$

Both p and $\boldsymbol{\omega}$ are independent in the direction of rotation, a quantity will be said to be rigid if it is axially invariant.

3. Results

We will now present a comparison against a benchmark 3D model of thermal convection (Figure 5). As mentioned before we wish to simulate the upper hemisphere of the shell. A few features we are trying to recover will be mentioned. Outside the TC, convection cell is in the prograde direction (Figure 5d). Reynolds stresses associated with these cells generate a zonal flow which is retrograde near the TC and prograde near the outermost boundary (Figure 5b). Inside the TC, we are able to observe axial plumes carrying heat through upwellings (Figure 5c,d). Close to the TC, the larger topographic effect and buoyancy leads to tilting of the convective cells. We are able to observe largest retrograde zonal flow occurs at the TC. These snapshots represent a benchmark of what the extended model should be able to replicate. Though we ran our QG model at different parameters: $E=10^{-4}$, $Ra=2-2.5 \times 10^7$, for computational reasons, we should be able to recover the main features of the full model. Before we continue with our comparison, I would also like to mention that we were able to find the critical Rayleigh number for the specified parameters to be 2.1×10^7 (Figure 6)

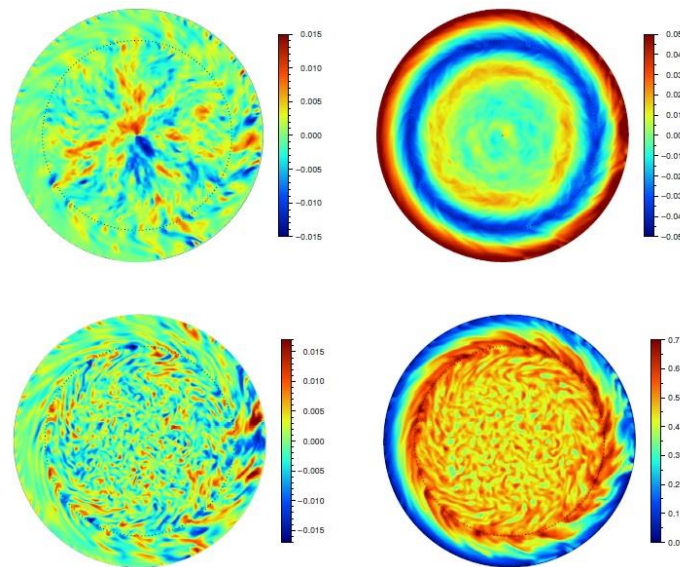


Figure 5. Snapshot of axially averaged quantities of the full 3D model. The parameters used are $r_i = 0.75$, $E=10^{-5}$, $Ra=4.8 \times 10^8$ and $Pr=1$, these parameters yield a fully turbulent flow. The tangent cylinder is represented by the black dashed line. Figure modified from Figure 5 Dumberry et al., 2015

a) Cylindrical radial flow; **b)** azimuthal flow; **c)** axial flow; **d)** Total temperature

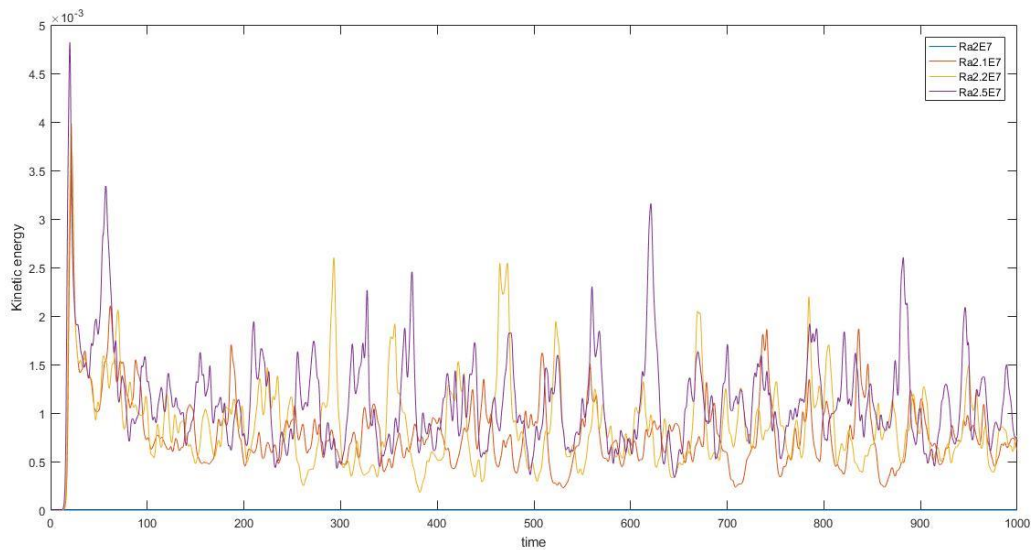


Figure 6. Kinetic energy for varying Ra. We can see that convection is sustained for values higher than 2E7 (Blue line). At 2E7 convection is not able to occur this the Kinetic energy rapidly decays to zero. This figure illustrates an intermittent convective regime with periodic outburst of energy.

Our experiment was usually run for about 10 hours, while the 3D model was ran for up to a couple of days. We are able to identify a few similarities between the extended and full model (Figure 7). First, outside the TC, non-rigid quantities should be zero and we observe that. Additionally, we can replicate similar amplitudes and spatial spectrum. Since only the poloidal flow is shown in Figure 7c, we are not able to replicate the connection between the rigid flow in the axial direction and radial flow. Furthermore, intermittent axial plumes are successfully replicates as seen in Figure 7c, again with similar amplitudes as the full model. The tilting of the convection cells near the TC are effectively reproduced. The azimuthal zonal wind also has similar amplitudes to the full model and we can also observe prograde flow outside the TC. Another recovered feature is the tilting of convection cells near the TC. When we focus our attention to the non-axisymmetric part of the rigid temperature, we can see thin thermal plumes (Figure 8).

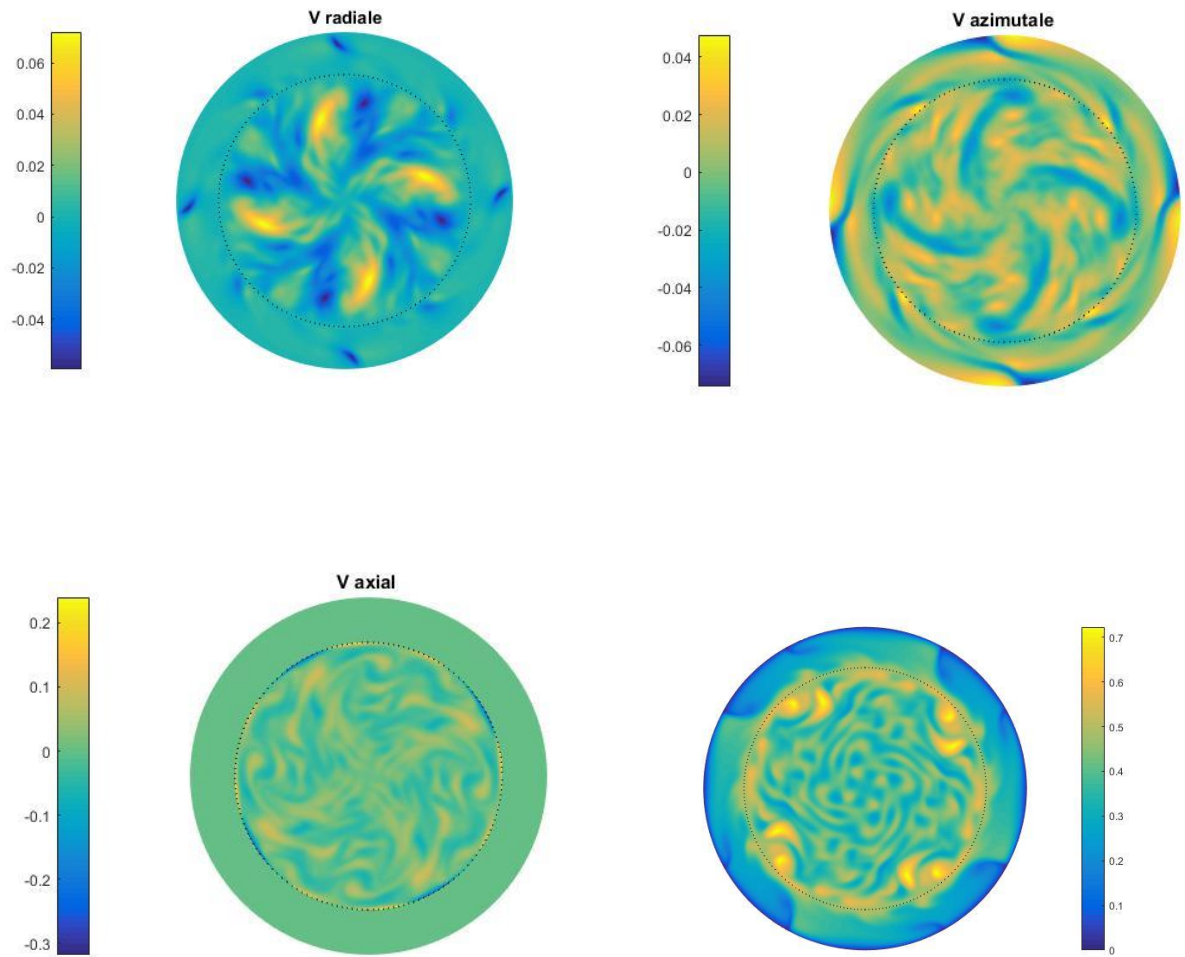


Figure 7. Snapshot of. The parameters used are $r_i = 0.75$, $E=10^{-4}$, $Ra=2.5 \times 10^7$ and $Pr=1$. The tangent cylinder is represented by the black dashed line.

a) Cylindrical radial flow; **b)** azimuthal flow; **c)** axial flow; **d)** Total temperature

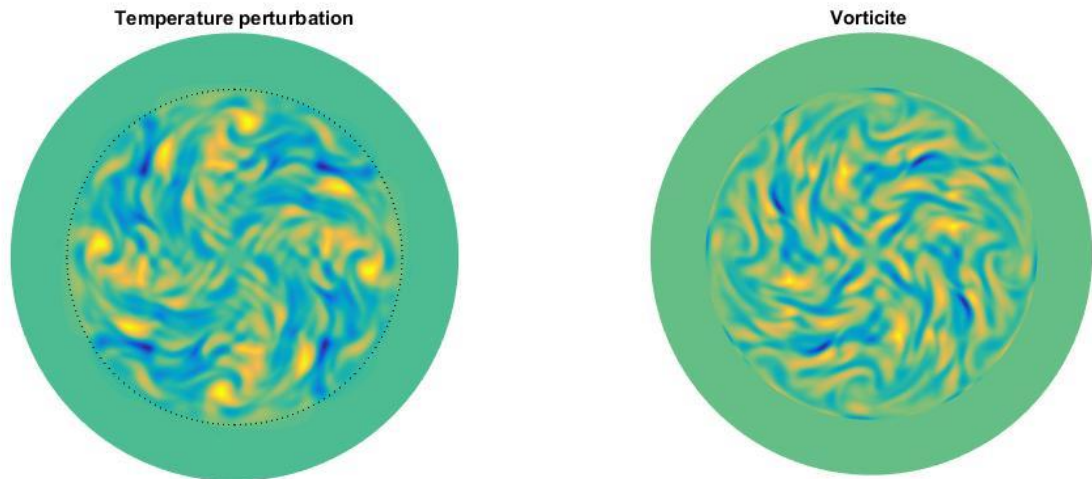


Figure 8. Snapshot in time

a) The non-axisymmetric rigid temperature perturbation; **b)** the non-rigid vorticity

4. Discussion

The goal was to decide whether the extended QG model for thermal convection developed by Dr. Dumberry and his team captures the first order dynamics inside and outside the TC. As previously mentioned, this required us to evolve and track both the rigid and non-rigid, anti-symmetric components of flow and temperature. For this particular model, quantities inside the tangent cylinder are represented by their axial gradient average. The extended model can be represented by a 2D problem since all quantities in a polar coordinate grid can be represented in an equatorial grid. A quick comparison demonstrates that the parameterized 2D model is able to reproduce the main features of thermal convection in a rapidly rotating shell. This is a step forward towards modeling full thermal convection at low computational cost.

5. Acknowledgments

I would like to thank Dr. Mathieu Dumberry for allowing me to do this project under his guidance, for always being available, extremely patient and willing to help. This project has grown my interest in Numerical models, their application on planetary bodies and computational efficiency. I would also like to thank Dr. Moritz for providing a full 3D benchmark model for comparison of

the results. Lastly, I would like to thank Daniel Laycock, a PhD student of Dr. Dumberry's group for extending these models to the region inside the tangent cylinder.

6. References

A. M. Soward. The Royal Society. Volume 275, issue 12560 (1974)

Andrew Soward. Convection, Nonmagnetic Rotating. Enciclopedia of Geomagnetism and Pelomagnetism. Pages 74-77 (2007)

Conrad, C. P. and C. Lithgow-Bertelloni, Science, v. 298, p. 207-209 (2002)

F. Sohl, M. Choukroun, J. Kargel et al. Space Sci Rev (2010)

G.W. Ojakangas, D.J. Stevenson, v. 66, Issue 2 (1986)

J. Aubert et al. Geochemistry, Geophysics, Geosystems. Volume 4, Issue 7 (2003)

J. Schmalzl, M. Breuer and U. Hansen. EPL, volume 67, Number 3 (2004)

Keke Zhang. Core Convection. Enciclopedia of Geomagnetism and Pelomagnetism. Pages 80-82 (2007)

Dumberry, Mathieu, Daniel Laycock, and Moritz Heimpel. "A generalized quasi-geostrophic model of thermal convection." EGU General Assembly Conference Abstracts. Vol. 17. 2015

*Proudman-Taylor Theorem. Enciclopedia of Geomagnetism and Pelomagnetism. Pages 852-853 (2007) (do again)

Savchenko, V. P. & Kozhevnikov, N. I. Soviet Astronomy, vol. 22, Page 459-464 (1978)

Krista M. Soderlund, J. M. Aurnoun. Americal Astronomical Society. Volume 39, Page 527